

# Part 1: clinoptilolite–alumina–hydroxyapatite composites for biomedical engineering

Cevriye Kalkandelen<sup>1,2</sup> · O. Gunduz<sup>3,4</sup> · A. Akan<sup>1,5</sup> · F. N. Oktar<sup>4,6</sup>

Received: 2 August 2016 / Revised: 1 September 2016 / Accepted: 14 September 2016 / Published online: 16 December 2016  
© Australian Ceramic Society 2016

**Abstract** The preparation and characterization of bovine hydroxyapatite (BHA) and clinoptilolite–alumina composites are studied. Clinoptilolite (Cp) and aluminium oxide ( $\text{Al}_2\text{O}_3$ ) (at varying concentrations 5, 10 and 15 wt% ) were added to calcinated BHA powder. Green cylindrical samples were sintered at several temperatures between 1000 and 1300 °C for 4 h in air. Compression strength, Vickers microhardness and elastic modulus, as well as density, were evaluated. Scanning electron microscopy (SEM), Fourier transform infrared spectroscopy (FTIR) and X-ray diffraction (XRD) studies were also performed. The experimental results showed that varying concentrations 5, 10 and 15 wt% Cp– $\text{Al}_2\text{O}_3$  to BHA and difference in the sintering temperature between 1000 and 1300 °C increase in the microhardness (67 and 305 HV, respectively), compression strength (between 31 and 105.6 MPa, respectively) and elastic modulus (between 540 and 1275 MPa, respectively). The experimental results gained

optimal parameters to be utilized in the preparation of BHA and Cp– $\text{Al}_2\text{O}_3$  composites. These natural Cp– $\text{Al}_2\text{O}_3$ /BHA composites have the potential to be used in several advanced biomedical engineering applications.

**Keywords** Bovine hydroxyapatite · Clinoptilolite · Alumina · Characterization · Biocomposites

## Introduction

Every year, millions of people suffer from a bone loss caused by trauma or illnesses. The standard treatment of bone defect comprise of in filling the bone defect with a material to support new bone structure. In most cases, autologous bone transplant is applied. Unfortunately, extracting this material needs a second surgery and may lead to complications for instance infections or long-lasting pains [1]. It is known that procedures involving bone materials conclude about 4,000,000 per annum globally [2]. Besides, the secondary graft source can be animal bones such as bovine-derived grafts. The production processes usually consist of freeze-dried method or preparation of the bone graft with diluted acids which may not be very safe since some deadly prions can survive the production processes. Since the 1980s research, prion diseases like mad cow disease have led to very serious results up to brain damage [3, 4]. Calcination method (850 °C) seems to be much better and safer when compared to the other methods underlined above [3, 4].

Although hydroxyapatite (HA) shows great biocompatibility, applications are limited to load-bearing areas and coatings, due to its low mechanical properties. These mechanical properties can be improved with addition of various materials [5, 6].

✉ Cevriye Kalkandelen  
kalkan@istanbul.edu.tr

<sup>1</sup> Biomedical Engineering Program, Istanbul University, Avcilar, 34320 Istanbul, Turkey  
<sup>2</sup> Vocational School of Technical Sciences, Biomedical Devices Technology Department, Istanbul University, 34320 Istanbul, Turkey  
<sup>3</sup> Department of Metallurgy and Materials Engineering, Faculty of Technology, Marmara University, Goztepe Campus, 34722 Istanbul, Turkey  
<sup>4</sup> Advanced Nanomaterials Research Laboratory (ANRL), Marmara University, Goztepe Campus, 34722 Istanbul, Turkey  
<sup>5</sup> Department of Electrical and Electronic Engineering, Istanbul University, Avcilar, 34320 Istanbul, Turkey  
<sup>6</sup> Department of Bioengineering, Faculty of Engineering, Marmara University, 34722 Istanbul, Turkey

In the world, there are more than 50 types of natural zeolites. Clinoptilolite (Cp) is one of the most widely used natural zeolite for medical and industrial application [7–9], as well as antibacterial agents [10].

There are few studies about HA–Zeolite composites presented in the literature. Iqbal et al. added 5, 10, 25 and 50 wt% zeolite to hydroxyapatite (HA). However, they processed HA and zeolite composites by using microwave synthesizing method. The nanostructured zeolite–HA composites they produced have resulted very good bioactivity and in vitro biocompatibility. This zeolite–HA may be considered potential candidates for bone tissue engineering applications [11]. Ceyhan et al. tested zeolites for stimulated body fluid for testing the bioactivity of zeolites as a biomaterial and obtained some encouraging results, including cell culture tests. It was observed that the lower and higher silicate and potassium content in zeolite did not affect the results of cell culture viability study [10]. Shainberg et al. compared zeolite and bone HA in terms of biomaterial properties [12]. Especially in some in vivo studies on dogs and rats, it was reported that several zeolite compounds have blocked the growth of some cancer cells [13].

Having SiO<sub>2</sub> and P<sub>2</sub>O<sub>5</sub> compositions in its structure, Cp shows similarity to bioglass (45S5) (bioglass includes as 45 wt% SiO<sub>2</sub>, 24.5 wt% Na<sub>2</sub>O, 24.5 wt% CaO and 6 wt% P<sub>2</sub>O<sub>5</sub>) [14]. There are many reviews in recent literature about the benefits of using original Hench's 45S5 bioglass and various bioglass types [15, 16]. Boron added bioglass reveals another large family of bioglasses (i.e. borat glasses) [17]. There are also some interesting studies about cell culture results of such boron (adding boron plays also an important role by manufacturing bioglass taking the very high temperatures from 1450 down to 950 °C added bioglasses tested by Valério et al. reporting on the increased bioactivity rates compared to other biomaterials, i.e. hydroxyapatite (HA) [18].

Alumina (Al<sub>2</sub>O<sub>3</sub>) is one of the most widely investigated materials, which are used as an ideal reinforcement oxide. It is also stated that when used the fine alumina, which effects on high strength [19]. Oktar et al. conducted a study adding 5–10 wt% Al<sub>2</sub>O<sub>3</sub> to BHA. Al<sub>2</sub>O<sub>3</sub> is typical representatives of inert bioceramics with very good mechanical performance [20]. It is also known that Al<sub>2</sub>O<sub>3</sub> leads to chemical inertness [21]. It has also been reported by Pavelić et al. that those aluminosilicate particulates interact with specific cells and modify their pathways [13].

In this study 5, 10 and 15 wt% Cp, and 5, 10 and 15 wt% Al<sub>2</sub>O<sub>3</sub> were mixed with bovine hydroxyapatite (BHA). Using the above compositions, compression (MPa), elastic modulus and Vickers microhardness (HV) samples were prepared and sintered between 1000 and 1300 °C. In addition, Archimedes densities, X-ray diffraction and scanning electron microscopy (SEM) studies were performed for the composites resulted

optimum mechanical tests. The aim of this study is to find out the most load resistant composite structure for future biomedical applications.

## Materials and methods

### Materials

In this study, femoral parts of bovine are used as BHA source. Bovine bones were collected from a chain store (CarrefourSA Haramidere, Istanbul, Turkey). It is known that this chain store never uses imported meat. In many EU reports, it is declared that mad cow disease is not detected in Turkey (up to 2007) [22]. “Rota Mining Company” Gordes, Izmir, supplied the Cp used in our experiments. The purity of mineral is about 90–95% (<40 μm). Foreign materials such as ferric oxide and mica were eliminated by using a magnetic field separator. The chemical analysis of the Cp is shown in Table 1. The Al<sub>2</sub>O<sub>3</sub> used in our composites was supplied by Alfa Aesar 42572 (<1 μm).

### Preparation of composites

Both heads of the femoral bones were cut off, and the bone marrow was taken out (Fig. 1a). The cleaned bone parts (Fig. 1a) were deproteinized with NaOH solution [23]. The bone parts were cleaned from chemicals under running water. After this process, the bone parts were subjected to calcination at 450 °C for 4 h (Fig. 1b), smashed into smaller pieces and sintered for 4 h up to 850 °C (Fig. 1c, d). The sintered BHA parts were grinded into smaller particles with wet ball milling and dried. BHA powders were sieved through a 75-μm sieve, and then mixed with 5, 10 and 15% in weight with Cp and Al<sub>2</sub>O<sub>3</sub> (the powder combinations of BHA–Cp–Al<sub>2</sub>O<sub>3</sub> are given in Table 2). These dried combinations were uniaxial pressed (at 350 MPa) to cylindrical pellets (11 mm of height and 11 mm in diameter) according to British Standards for compression tests [2], number 7253 [24, 25]. The pressed BHA composite green bodies were sintered between 1000 and 1300 °C for 4 h [2].

### Characterization of clinoptilolite–alumina–bovine hydroxyapatite composites

The mechanical properties were evaluated using a universal compression-testing (with 2 mm/min displacement) machine DVT (Devotrans Inc., Istanbul, Turkey). Vickers microhardness (HV) test was conducted at 200-g load with 20 s of dwell time (Shimadzu HMV-2, Kyoto, Japan). The density of sintered samples was applied using an Archimedes method. Scanning electron microscopy (SEM) (Jeol 590, Tokyo, Japan), X-ray diffraction tests

**Table 1** Chemical analysis of the Cp

Molecule	SiO <sub>2</sub>	Al <sub>2</sub> O <sub>3</sub>	Fe <sub>2</sub> O <sub>3</sub>	MgO	CaO	MnO	P <sub>2</sub> O <sub>5</sub>	K <sub>2</sub> O	Na <sub>2</sub> O	SO <sub>3</sub>	TiO <sub>2</sub>	Loss of ignition	Σ
Cp	66.77	11.86	1.44	1.48	4.30	0.04	0.04	2.39	0.14	0.02	0.11	11.2	99.72

(XRD) (XRD-6000, Shimadzu, Kyoto, Japan) and Fourier transform infrared spectroscopy (FTIR) tests (AIM-8800, Shimadzu, Kyoto, Japan) were performed to analyse microstructure and phases.

## Results and discussions

Table 2 reveals the densities and compression strength (MPa) of various samples fabricated using different concentrations of Cp and Al<sub>2</sub>O<sub>3</sub> along with the sintering temperatures. For all samples, as the sintering temperature of each concentration is increased, the density is increased as well. In all cases, when the sintering temperature is increased to 1000 to 1300 °C, the density is increased by 10–20 wt%. Hence, for each specific sintering temperature, the density of each sample concentration is equivalent. Sintering method is the most crucial phase in ceramic powder processing used to produce density-controlled ceramic, causing the particles to form bonds that are needed to hold mass together during very high temperature [26].

In previous work, Oktar et al. conducted compression strength and microhardness testing for sintered synthetic hydroxyapatite. The highest compressive strength of 30.47 MPa (1100 °C) and 29.13 MPa (1300 °C) were obtained [27].

Goller et al. used a similar study but using BHA instead of using synthetic hydroxyapatite. The best compression strengths were of result 67 (1200 °C) and 62 MPa (1300 °C) [28]. Oktar et al. prepared Al<sub>2</sub>O<sub>3</sub> with BHA composites. The highest compressive strength for 10 wt% Al<sub>2</sub>O<sub>3</sub> content was in the range 87.81 MPa (1300 °C) [20].

Demirkol et al. utilized a similar study adding 5–10 wt% commerce inert glass (CIG) to synthetic sheep-derived HA (SHA) and synthetic hydroxyapatite (HA). The best compressive strength of 76 MPa value was obtained by 5 wt% CIG in addition to SHA as 76 MPa. The best compression strength value was obtained by 5 wt% CIG addition to HA as 95 MPa [29].

Table 2 shows the compression strength of various BHA composites (5, 10 and 15 wt% Cp and Al<sub>2</sub>O<sub>3</sub>) prepared at different temperatures (1000, 1100, 1200 and 1300 °C). The maximum value for compression strength was found for samples prepared at 1300 °C in the order 15 wt% Cp–15 wt% Al<sub>2</sub>O<sub>3</sub> (105.6 MPa). Although there is a big difference between 5 and 10 wt% Cp and Al<sub>2</sub>O<sub>3</sub> samples results in compression strengths that are significantly higher than samples containing the low concentration of Cp and Al<sub>2</sub>O<sub>3</sub> by over 31 MPa. The elastic modules behaved in a similar manner to the compression strength the highest value (1275 MPa) obtained in the 15 wt% Cp–15 wt% Al<sub>2</sub>O<sub>3</sub> in Table 3.

**Fig. 1** Preparation of BHA. **a** The cleaned bone parts with NaOH (sodium hydroxide) solution. **b** After cleaning process, the bone parts were calcinated at 450 °C for 4 h. **c, d** After the bone parts were calcinated at 850 °C for 4 h

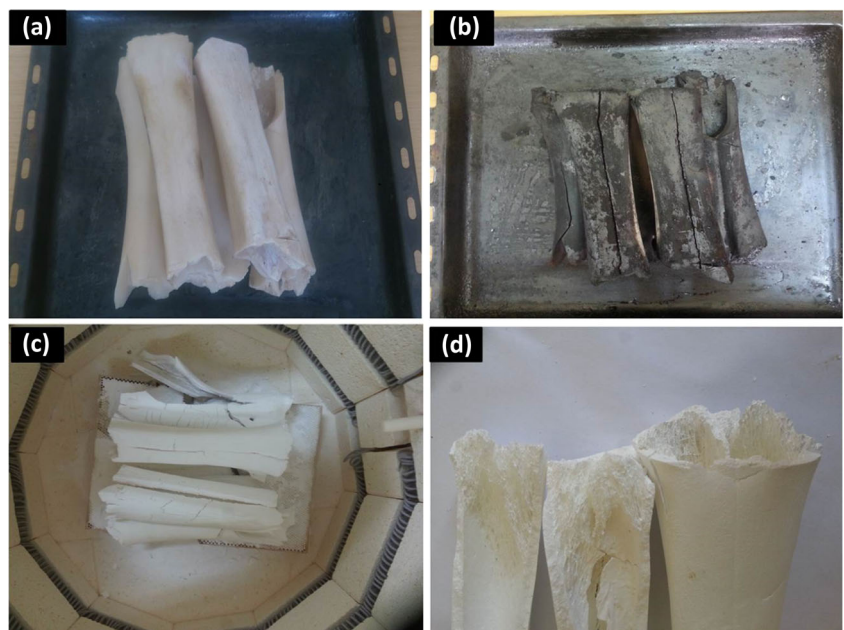


**Table 2** Influence of Cp and Al<sub>2</sub>O<sub>3</sub> content (5, 10 and 15 wt%) on density and compression strength (MPa) of Cp–Al<sub>2</sub>O<sub>3</sub>–BHA composites at different temperatures

T [°C]	5 wt% Cp–5 wt% Al <sub>2</sub> O <sub>3</sub> –BHA		10 wt% Cp–5 wt% Al <sub>2</sub> O <sub>3</sub> –BHA		5 wt% Cp–10 wt% Al <sub>2</sub> O <sub>3</sub> –BHA		10 wt% Cp–10 wt% Al <sub>2</sub> O <sub>3</sub> –BHA		15 wt% Cp–15 wt% Al <sub>2</sub> O <sub>3</sub> –BHA		15 wt% Cp–10 wt% Al <sub>2</sub> O <sub>3</sub> –BHA	
	d (gr/cm <sup>3</sup> )	σ (MPa)	d (gr/cm <sup>3</sup> )	σ (MPa)	d (gr/cm <sup>3</sup> )	σ (MPa)	d (gr/cm <sup>3</sup> )	σ (MPa)	d (gr/cm <sup>3</sup> )	σ (MPa)	d (gr/cm <sup>3</sup> )	σ (MPa)
1000	1.886 ± 0.011	31.0 ± 4.5	1.893 ± 0.024	39.0 ± 9.3	1.885 ± 0.029	37.6 ± 5.8	1.825 ± 0.028	40.2 ± 5.3	1.771 ± 0.030	41.8 ± 4.6	1.789 ± 0.029	38.4 ± 7.1
1100	1.925 ± 0.018	37.2 ± 4.6	1.913 ± 0.053	44.6 ± 5.6	1.943 ± 0.053	44.8 ± 4.8	1.834 ± 0.012	45.6 ± 7.8	1.808 ± 0.018	45.6 ± 5.7	1.799 ± 0.017	44.4 ± 6.2
1200	2.009 ± 0.046	49.0 ± 6.2	2.021 ± 0.027	51.0 ± 7.6	2.064 ± 0.022	72.2 ± 9.8	2.106 ± 0.011	62.6 ± 9.1	2.061 ± 0.022	90.2 ± 11.5	2.160 ± 0.030	78.6 ± 8.5
1300	2.219 ± 0.074	53.4 ± 8.9	2.403 ± 0.054	70.2 ± 10.9	2.369 ± 0.088	94.8 ± 12.6	2.548 ± 0.038	96.0 ± 13.8	2.337 ± 0.018	105.6 ± 15.2	2.270 ± 0.092	99.4 ± 12.3

**Table 3** Microhardness measurements (HV) and elastic modulus (MPa) of BHA–Cp–Al<sub>2</sub>O<sub>3</sub> composites

T [°C]	5 wt% Cp–5 wt% Al <sub>2</sub> O <sub>3</sub> –BHA		10 wt% Cp–5 wt% Al <sub>2</sub> O <sub>3</sub> –BHA		5 wt% Cp–10 wt% Al <sub>2</sub> O <sub>3</sub> –BHA		10 wt% Cp–10 wt% Al <sub>2</sub> O <sub>3</sub> –BHA		15 wt% Cp–15 wt% Al <sub>2</sub> O <sub>3</sub> –BHA		15 wt% Cp–10 wt% Al <sub>2</sub> O <sub>3</sub> –BHA	
	HV	E (MPa)	HV	E (MPa)	HV	E (MPa)	HV	E (MPa)	HV	E (MPa)	HV	E (MPa)
1000	67 ± 12.7	540 ± 61	82 ± 14.0	605 ± 48	88 ± 10.5	767 ± 58	86.1 ± 17.4	703 ± 54	94 ± 23.4	605 ± 78	90 ± 23.4	556 ± 52
1100	74 ± 14.1	599 ± 78	99 ± 16.3	754 ± 69	116 ± 18.5	788 ± 79	121 ± 20.1	787 ± 81	135 ± 26.6	767 ± 98	119 ± 24.4	627 ± 83
1200	144 ± 22	823 ± 83	131 ± 16.8	937 ± 82	175 ± 40.5	892 ± 89	182 ± 31.1	954 ± 105	220 ± 38.7	987 ± 109	175 ± 40.5	959 ± 128
1300	166 ± 24.7	973 ± 96	169 ± 24.9	1058 ± 99	185 ± 45.0	1003 ± 94	266 ± 44.7	1156 ± 129	305 ± 56.0	1275 ± 112	225 ± 55.0	1088 ± 131

The best results for microhardness (Table 3) were measured at 15 wt% Cp–15 wt%  $\text{Al}_2\text{O}_3$  content at 1300 °C (305 HV). By comparison, this is also relative to density values at the sintering temperature ( $2.337 \text{ g/cm}^3$ ), showing that compression strength is also affected by density, despite the fact that this is not the only factor [2]. It is clearly known that Cp and  $\text{Al}_2\text{O}_3$  are natural material and there are limited studies in the previous studies relating to it as a bioceramic composite with hydroxyapatite. So, when comparing compression strength and microhardness values of composite BHA and BHA merely, (Tables 2 and 3) the doping role of Cp and  $\text{Al}_2\text{O}_3$  becomes intensely valuable.

X-ray powder diffraction patterns of the starting pure BHA,  $\text{Al}_2\text{O}_3$ , natural clinoptilolite and varying composite of BHA are shown in Figs. 2 and 3. Figure 2c was clearly indicated that it was similar to the hydroxyapatite standard XRD pattern of the sample BHA [4]. The main XRD peaks of clinoptilolite are generally observed at 11.190, 130, 17.50, 22.430, 26.80 and 30.500 in Fig. 2b [30]. The XRD pattern of the as obtained  $\text{Al}_2\text{O}_3$  powders (Fig. 2a) shows the reference XRD pattern (42–1468 JCPDS file).

XRD patterns of samples are shown in Fig. 3. Varying Cp and  $\text{Al}_2\text{O}_3$  reinforcement concentrations (5, 10 and 15 wt%) and sintering temperatures (1000 and 1300 °C) are revealed.

Figure 3a and b presents the XRD patterns of 5 wt% Cp–5 wt%  $\text{Al}_2\text{O}_3$ /BHA composite samples, exhibiting strong diffraction peaks belonging to the hydroxyapatite (JCPDS card number: 98-008-9679) and whitlockite (JCPDS card number: 98-000-2071) stable phases. Furthermore, whitlockite phase amount decreases sharply with increasing sintering temperature. Cp are observed at 22.430 and 30.500  $2\theta$ . In addition, three peaks at 34.90, 43.20 and 57.50 were attributed to the characteristic peaks of  $\text{Al}_2\text{O}_3$  [31], indicating the corporation of  $\text{Al}_2\text{O}_3$  and clinoptilolite into BHA. Figure 3c and d shows the XRD patterns of 10 wt% Cp and 5 wt%  $\text{Al}_2\text{O}_3$ /BHA composite samples. It is also obvious that hydroxyapatite, tricalcium bis(orthophosphate), whitlockite, Cp and  $\text{Al}_2\text{O}_3$  stable phases peaks were clearly observed. Cp phase amount increases sharply with increasing sintering temperature from 1000 to 1300 °C. Moreover, tricalcium bis(orthophosphate) and Cp phase amount increase gradually with increasing sintering temperature and increase in phosphate peak height after sintering process. 5 wt% Cp–10wt%  $\text{Al}_2\text{O}_3$ /BHA composite samples consisting of diffraction peaks belonging to hydroxyapatite, tricalcium bis(orthophosphate), whitlockite, Cp and  $\text{Al}_2\text{O}_3$  phases depending upon sintering temperature changing between 1000 and 1300 °C are revealed in Fig. 3e and f. Figure 3g and h reveals the XRD patterns of 10 wt% Cp and

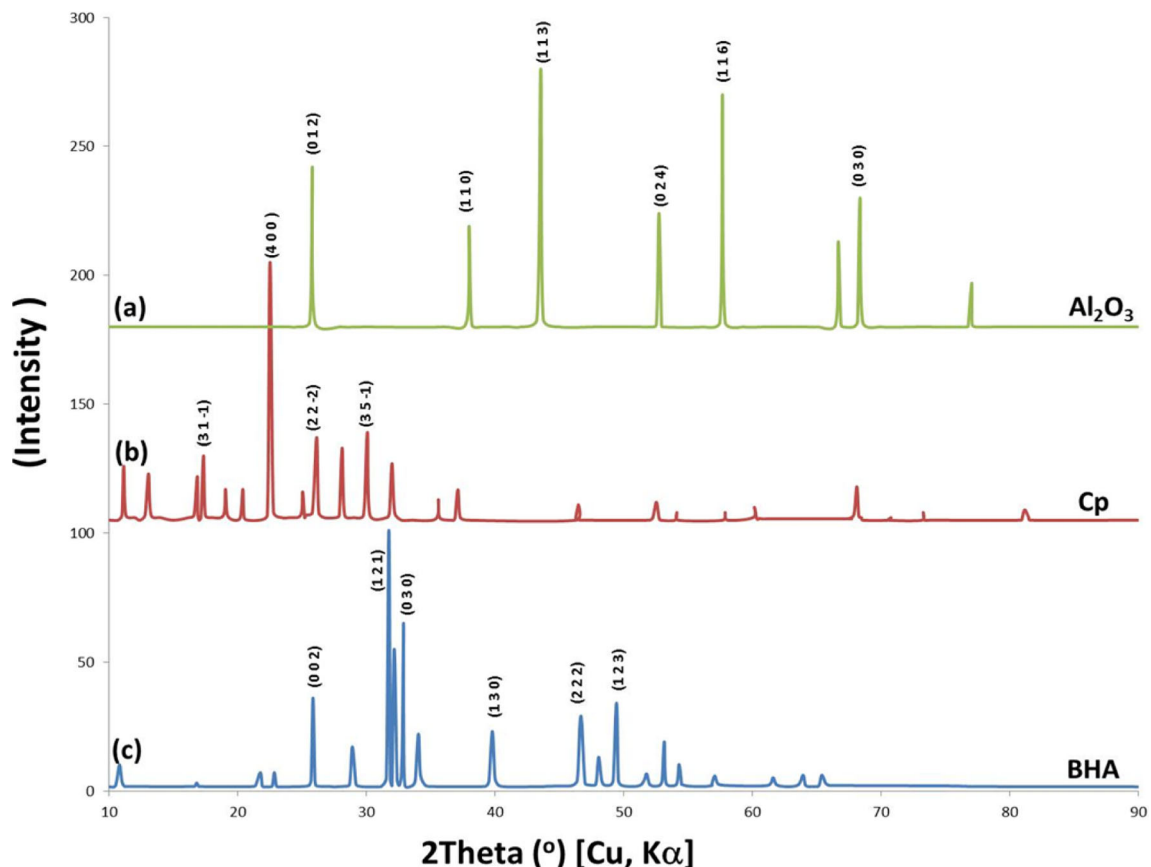


**Fig. 2** X-ray diffractograms of raw materials (unprocessed). **a**  $\text{Al}_2\text{O}_3$ . **b** Cp. **c** BHA

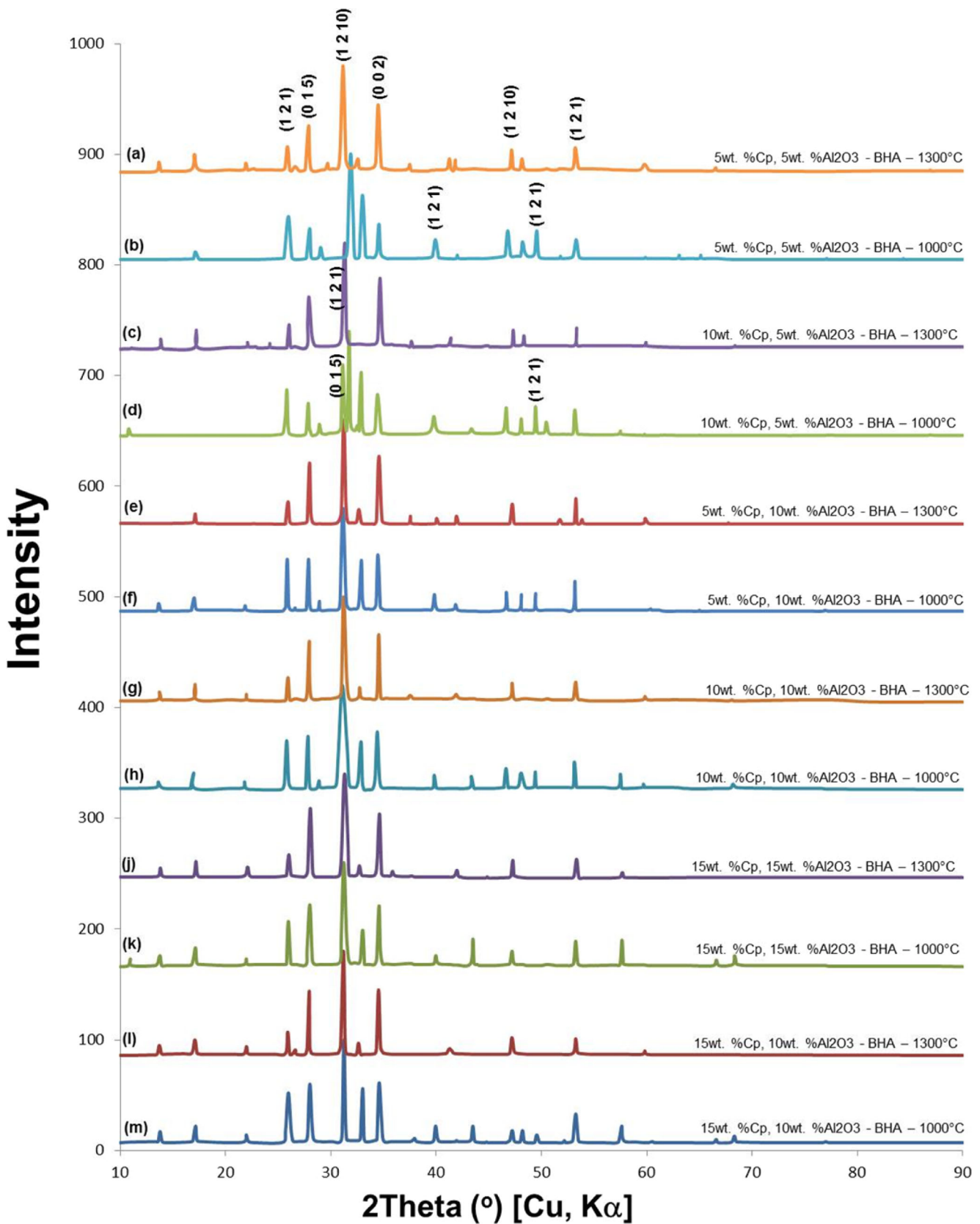


**Fig. 3** X-ray diffractograms of BHA composites doped with **a, b** 5 wt% of Cp–5 wt% of Al<sub>2</sub>O<sub>3</sub> at 1300 and 1000 °C. **c, d** 10 wt% of Cp–5 wt% of Al<sub>2</sub>O<sub>3</sub> at 1300 and 1000 °C. **e, f** 5 wt% of Cp–10 wt% of Al<sub>2</sub>O<sub>3</sub> at 1300

and 1000 °C. **g, h** 10 wt% of Cp–10 wt% of Al<sub>2</sub>O<sub>3</sub> at 1300 and 1000 °C. **j, k** 15 wt% of Cp–15 wt% of Al<sub>2</sub>O<sub>3</sub> at 1000 and 1000 °C. **l, m** 15 wt% of Cp–10 wt% of Al<sub>2</sub>O<sub>3</sub> at 1300 and 1000 °C

10 wt%  $\text{Al}_2\text{O}_3$ /BHA composite samples. It is noticeable that hydroxyapatite, tricalcium bis(orthophosphate), whitlockite, clinoptilolite and  $\text{Al}_2\text{O}_3$  phases peaks were indicated. Also, whitlockite (JCPDS card number: 98-008-0800) phase amount increases gradually with increasing temperature and increases in Cp and  $\text{Al}_2\text{O}_3$  peak height after sintering heat treatment. 15 wt%  $\text{Al}_2\text{O}_3$ –15 wt% Cp/BHA composite samples consisting of diffraction peaks belonging to tricalcium bis(orthophosphate), whitlockite, clinoptilolite and  $\text{Al}_2\text{O}_3$  phases depending upon sintering temperature changing between 1000 and 1300 °C are revealed in Fig. 3h and j. Although any new phase was not observed in the samples for 15 wt% clinoptilolite–10 wt%  $\text{Al}_2\text{O}_3$ –BHA in Fig. 3l and m.

Observation of the microstructure of the sintered samples, typically indicated in the SEM images of Figs. 4 and

5, reveals that trend. Specifically, a high densification regime is suggested after sintering at 1300 °C whereas rather a poor densification characterizes the samples sintered at 1000 °C. A peculiar microstructure was revealed after sintering 1300 °C (Fig. 4b–f). Especially, at the high temperature, cubic-like configuration converted. Similar structures were also observed in the SEM images of Fig. 5b–f, which correspond to higher than 10 wt% of Cp– $\text{Al}_2\text{O}_3$ –BHA powder composite sintered at 1300 °C. Perfect grain growth of 1300 °C sintered higher than 10 wt% doping with BHA was notable at low and high magnification (Fig. 5a–f). From the SEM images, samples containing 15 wt% Cp– $\text{Al}_2\text{O}_3$  demonstrate the best compromise between quantity and uniform distribution (reduced clustering).

**Fig. 4** SEM images of the BHA composites doped with **a, b** 5 wt% of Cp–5 wt% of  $\text{Al}_2\text{O}_3$  at 1300 and 1000 °C. **c, d** 10 wt% of Cp–5 wt% of  $\text{Al}_2\text{O}_3$  at 1000 and 1300 °C. **e, f** 5 wt% of Cp–10 wt% of  $\text{Al}_2\text{O}_3$  at 1000 and 1300 °C; the corresponding low magnification ( $\times 1000$ ) SEM images

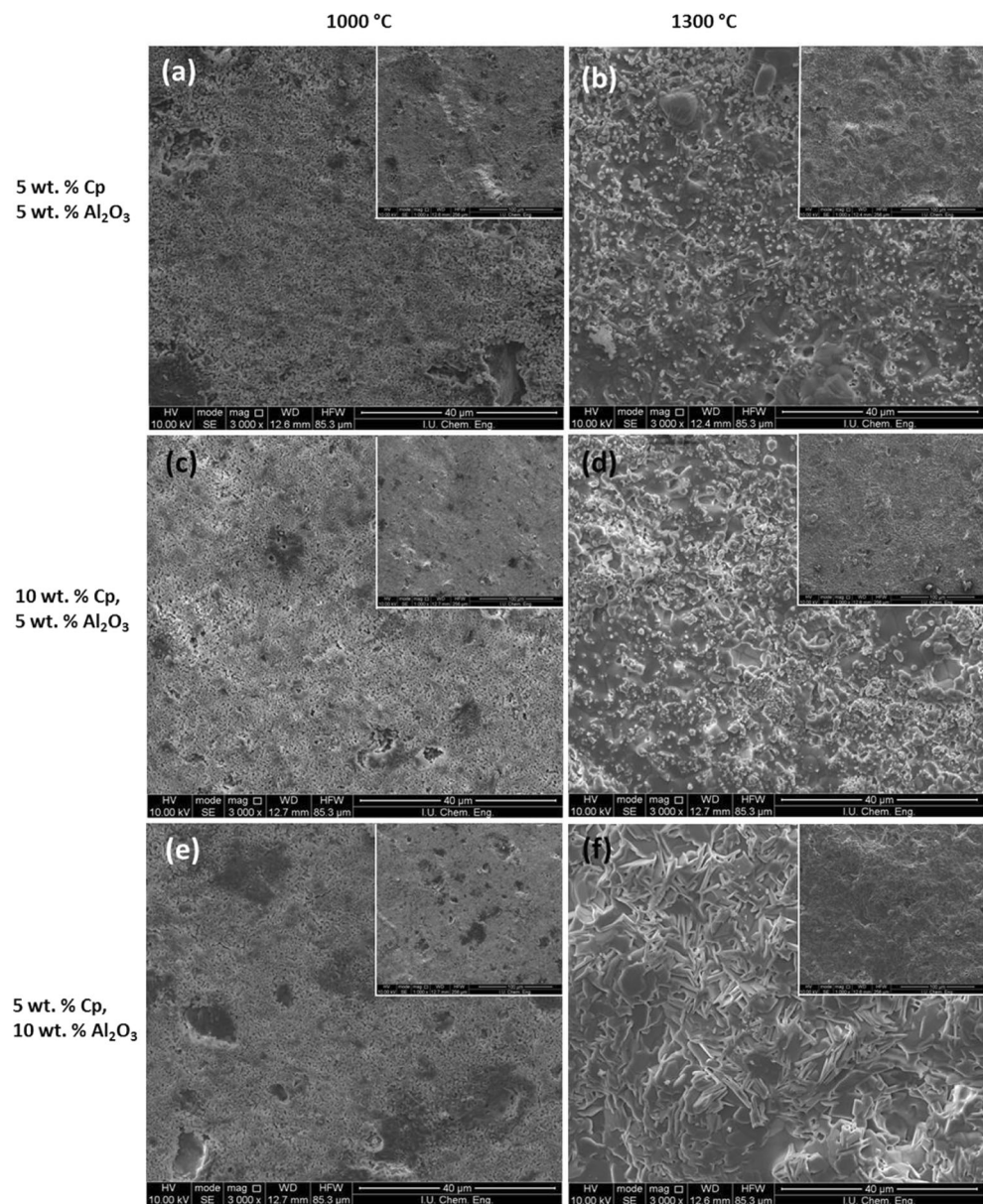
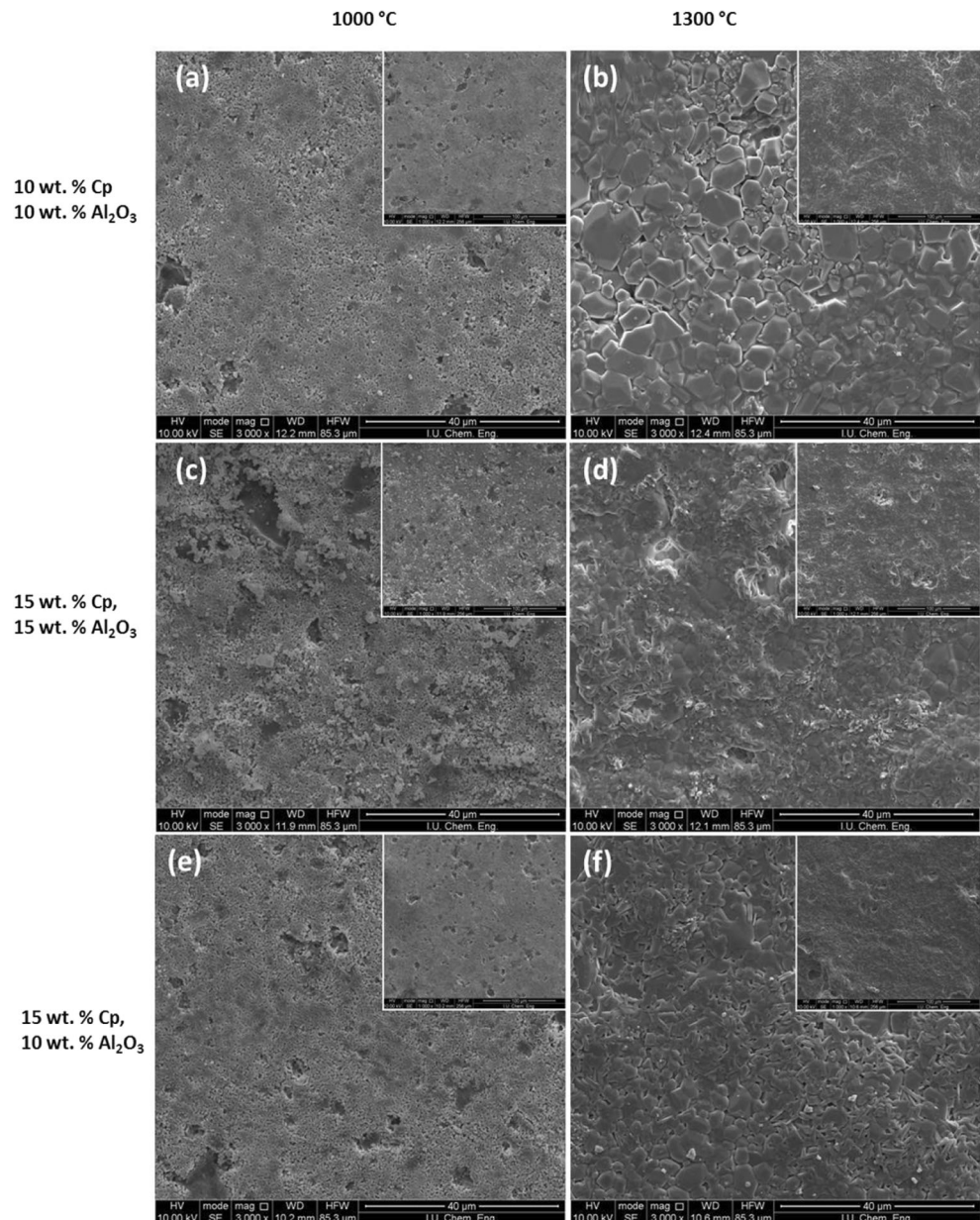


**Fig. 5** SEM images of the BHA composites doped with **a, b** 10 wt% of Cp–10 wt% of  $\text{Al}_2\text{O}_3$  at 1000 and 1300 °C. **c, d** 15 wt% of Cp–15 wt% of  $\text{Al}_2\text{O}_3$  at 1000 and 1300 °C. **e, f** 15 wt% of Cp–10 wt% of  $\text{Al}_2\text{O}_3$  at 1000 and 1300 °C; the *insets* showing corresponding low magnification ( $\times 1000$ ) SEM images



## Conclusions

It is seen that the increase of density is proportional to increase of  $\text{Al}_2\text{O}_3$  and reverse proportional with increase of heat. While the increase of  $\text{Al}_2\text{O}_3$  the microhardness, compression and elastic modulus values were increasing the hardness, it is detected that those values did not interfere with increasing of Cp content at lower temperatures. The optimum microhardness values were obtained at 10% equal composition value and at 1300 °C heat. It is seen, if the increase of  $\text{Al}_2\text{O}_3$  and or Cp exceeded over 10%, the mechanical values were decreasing. BHA–Cp composites are presenting mechanical values with bioglass composites. Beside all this, the biocompatibility test must be conducted.

**Acknowledgements** This study was supported by Istanbul University, Scientific Research Projects Coordination Unit, Project No: 29071.

## References

1. Bohner, M., Tadier, S., van Garderen, N., de Gasparo, A., Döbelin, N., Baroud, G.: Synthesis of spherical calcium phosphate particles for dental and orthopedic applications. *Biomatter*. **3**, e25103 (2013). doi:[10.4161/biomatter.25103](https://doi.org/10.4161/biomatter.25103)
2. Gunduz, O., Gode, C., Ahmad, Z., Gökçe, H., Yetmez, M., Kalkandelen, C., Sahin, Y.M., Oktar, F.N.: Preparation and evaluation of cerium oxide-bovine hydroxyapatite composites for biomedical engineering applications. *J Mech Behav Biomed Mater*. **35**, 70–76 (2014)



3. Goller, G., Oktar, F.N., Ozyegin, L.S., Kayali, E.S., Demirkesen, E.: Plasma-sprayed human bone-derived hydroxyapatite coatings: effective and reliable. *Mater Lett.* **58**(21), 2599–2604 (2004)
4. Ozyegin, L.S., Oktar, F.N., Goller, G., Kayali, E.S., Yazici, T.: Plasma-sprayed bovine hydroxyapatite coatings. *Mater Lett.* **58**(21), 2605–2609 (2004)
5. Oktar, F.N., Göller, G.: Sintering effects on mechanical properties of glass-reinforced hydroxyapatite composites. *Ceram Int.* **28**(2), 617–621 (2002)
6. Erkmén, Z.E., Genç, Y., Oktar, F.N.: The microstructural and mechanical properties of hydroxyapatite-zirconia composites. *J Am Ceram Soc.* **9**(90), 2885–2892 (2007)
7. Bogdanov, B., Georgiev, D., Angelova, K., Yaneva, K.: Natural zeolites: clinoptilolite, review. International science conference 4th -5th June 2009, Stara Zagora, Bulgaria. Economics and Society development on the Base of Knowledge. **4**, 6–11 (2009)
8. Nishihara, H., Kyotani, T.: Zeolite-Templated Carbon—Its Unique Characteristics and Applications, Novel Carbon Adsorbents Chapter 10. Elsevier, Amsterdam (2012)
9. Gazi, N.A., Malek, N.A.N.N., Hamdan, S.: Cytostatic activity of clinoptilolite against human cervical cancer cell lines using three different media-sterilization techniques. *Adv Mater Res (Dumten-Zurich, Switz).* **626**, 667–671 (2013)
10. Ceyhan, T., Tatlier, M., Akçakaya, H.: In vitro evaluation of the use of zeolites as biomaterials: effects on simulated body fluid and two types of cells. *J Mater Sci Mater Med.* **18**, 1557–1562 (2007)
11. Iqbal, N., Kadir, M.R.A., Mahmood, N.H.B., Yusoff, M.F.M., Siddique, J.A., Salim, N., Froemming, G.R.A., Sarian, M.N., Raghavendran, H.R.B., Kamarul, T.: Microwave synthesis, characterization, bioactivity and in vitro biocompatibility of zeolite-hydroxyapatite (Zeo-HA) composite for bone tissue engineering applications. *Ceram Int.* **40**, 16091–16097 (2014)
12. Schainberg, A.P.M., Ozyegin, L.S., Kursuoğlu, P., Valerio, P., Goes, A.M., Leite, M.F.: Biocompatibility evaluation of zeolite compared to bone HA, calcium phosphate ( $\text{Ca}_2\text{PO}_4$ ) and eugenol paste. *Key Eng Mater.* **284-286**, 561–564 (2005)
13. Pavelić, K., Hadžija, M., Bedrica, L., Pavelić, J., Diki, I., Katić, M., Kralj, M., Bosnar, M.H., Kapitanović, S., Poljak-Blaži, M., Križanac, Š., Stojković, R., Jurin, M., Subotić, B., Čolić, M.: Natural zeolite clinoptilolite: new adjuvant in anticancer therapy. *J Mol Med.* **78**, 708–720 (2001)
14. Goller, G., Yazici, T., Oktar, F.N., Demirkesen, E., Kayali, E.S.: Analysis of in-vitro reaction layers formed on plasma sprayed bioglass-titanium coatings. *Key Eng Mater.* **264-268**, 1973–1976 (2004)
15. Hoppe, A., Güldal, N.S., Boccaccini, A.R.: A review of the biological response to ionic dissolution products from bioactive glasses and glass-ceramics. *ACS Biomater Sci Eng.* **32**, 2757–2774 (2011)
16. Jones, J.R.: Review of bioactive glass: from Hench to hybrids. *Acta Biomater.* **9**, 4457–4486 (2013)
17. Bi, L., Rahaman, M.N., Day, D.E., Brown, Z., Samujh, C., Liu, X., Mohammadkhan, A., Dusevich, V., Eick, J.D., Bonewald, L.F.: Effect of bioactive borate glass microstructure on bone regeneration, angiogenesis, and hydroxyapatite conversion in a rat calvarial defect model. *Acta Biomater.* **9**, 8015–8026 (2013)
18. Valério, P., Goes, A.M., Karacayli, U., Gunduz, O., Salman, S., Sengil, A.Z., Yılmaz, S., Agathopoulos, S., Oktar, F.N.: Influence of Boroxide Bioactive Bioglasses (BBB) on Osteoblast Viability, Biodental Engineering. CRC Press/Balkema, Leiden (2010)
19. Ebrahimi, M., Ebadzadeh, T., Salah, E.: Effect of sintering atmosphere on phase evolution of hydroxyapatite nanocomposite powders. Proceedings of the International Conference Nanomaterials: Applications and Properties, vol. 1, no. 2 (2012). 02NNBM05(3 pp)
20. Oktar, F.N., Agathopoulos, S., Ozyegin, L.S., Gunduz, O., Demirkol, N., Bozkurt, Y., Salman, S.: Mechanical properties of bovine hydroxyapatite (BHA) composites doped with  $\text{SiO}_2$ ,  $\text{MgO}$ ,  $\text{Al}_2\text{O}_3$ , and  $\text{ZrO}_2$ . *J Mater Sci Mater Med.* **18**, 2137–2143 (2007)
21. Family, R., Solati-Hashji, M., Nik, S.N., Nemati, A.: Surface modification for titanium implants by hydroxyapatite nanocomposite. *Caspian J Intern Med.* **3**(3), 460–465 (2012)
22. Karacayli, U., Gunduz, O., Salman, S., Ozyegin, L.S., Agathopoulos, S., Oktar, F.N.: Effect of sintering temperature on mechanical properties and microstructure of sheep-bone derived hydroxyapatite (SHA). 13. International Conference on Biomedical Engineering IFMBE Proceedings. **23**, 1271–1274 (2008)
23. Goller, G., Oktar, F.N.: Sintering effects on mechanical properties of biologically derived dentine hydroxyapatite. *Mater Lett.* **56**(3), 142–147 (2002)
24. Goller, G., Oktar, F.N.: Effects of sintering on mechanical properties of biologically derived hydroxyapatite. *Key Eng Mater.* **206**(2), 1615–1619 (2002)
25. Oktar, F.N., Meydanoglu, O., Goller, G., Agathopoulos, S., Rocha, G., Ozyegin, S., Eruslu, N., Peker, I., Kayali, S.: Sintering effects on mechanical properties of hydroxyapatite-titanium dioxide ( $\text{HA-TiO}_2$ ) composites. *Key Eng Mater.* **309-311**, 355–358 (2006)
26. Bernard-Granger, G., Guizard, C., San-Mihuel, L.: Sintering behaviour and optical properties of yttria. *J Am Ceram Soc.* **90**(9), 2698–2702 (2007)
27. Oktar, F.N., Genç, Y., Göller, G., Erkmén, E.Z., Özyeğin, L.S., Toykan, D., Demirkiran, H., Haybat, H.: Sintering of synthetic hydroxyapatite compacts. *Key Eng Mater.* **264-268**, 2087–2090 (2004)
28. Goller, G., Oktar, F.N., Agathopoulos, S., Tulyaganov, D.U., Ferreira, J.M.F., Kayali, E.S., Peker, I.: Effect of sintering temperature on mechanical and microstructural properties of bovine hydroxyapatite (BHA). *J Sol-Gel Sci Technol.* **2**(37), 111–115 (2006)
29. Demirkol, N.: Production and characterization of sheep hydroxyapatite composites, PhD; Istanbul Technical University Turkey (2013)
30. Copcia, V.E., Luchian, C., Dunca, S., Bilba, N., Hristodor, C.M.: Antibacterial activity of silver-modified natural clinoptilolite. *J Mater Sci.* **46**, 7121–7128 (2011)
31. Epure, L.M., Dimitrievska, S., Merhi, Y., Yahia, L.H.: The effect of varying  $\text{Al}_2\text{O}_3$  percentage in hydroxyapatite/ $\text{Al}_2\text{O}_3$  composite materials: morphological, chemical and cytotoxic evaluation. *J Biomed Mater Res, Part A.* **83A**(4), 1009–1023 (2007)